Not a benign motor neuron disease: longitudinal imaging captures relentless motor connectome disintegration in Primary Lateral Sclerosis

Marlene Tahedl[1], Ee Ling Tan[1], Stacey Li Hi Shing[1], Rangariroyashe H. Chipika[1], We Fong Siah[1], Jennifer C. Hengeveld[2], Mark A. Doherty[2], Russell L. McLaughlin[2], Orla Hardiman[1], Eoin Finegan[1]*, Peter Bede [1,3]*

Institutional affiliations

[1] Computational Neuroimaging Group (CNG), Biomedical Sciences Institute, Trinity College Dublin, Ireland

[2] Smurfit Institute of Genetics, Trinity College Dublin, Dublin, Ireland

[3] Department of Neurology, St James's Hospital, Dublin, Ireland

* Joint senior authors

Corresponding author: Peter Bede **Address**: Room 5.43, Computational Neuroimaging Group (CNG), Trinity Biomedical Sciences Institute, Trinity College Dublin, Pearse Street, Dublin 2, Ireland. **E-mail**: bedep@tcd.ie

Conflicts of interest statement: None of the authors have a conflict of interest to disclose

Tables: 2

Figures: 6

References: 50

Abstract word count: 243

Manuscript word count: 3499

Keywords: Primary Lateral Sclerosis, Biomarkers, Motor neuron disease, Neuroimaging, Clinical trials, Connectivity

Running title: Motor connectome disintegration in PLS

This article has been accepted for publication and undergone full peer review but has not been through the copyediting, typesetting, pagination and proofreading process which may lead to differences between this version and the Version of Record. Please cite this article as doi: 10.1111/ene.15725

Abstract

Introduction: Primary Lateral Sclerosis (PLS) is a low-incidence, progressive upper motor neuron disorder associated with considerable clinical disability. Disability is typically exclusively linked to primary motor cortex degeneration and the contribution of pre- and supplementary motor regions, somatotopic cortical-medullary and inter-hemispheric connectivity alterations are less well characterised.

Methods: In a single-centre, prospective, longitudinal neuroimaging study 41 patients with PLS were investigated. Patients underwent standardised neuroimaging, genetic profiling with whole exome sequencing, and comprehensive clinical assessments including UMN scores, tapping rates, mirror movements, spasticity assessment, cognitive screening and evaluation for pseudobulbar affect. Longitudinal neuroimaging data from 108 healthy controls were used for image interpretation. A standardised imaging protocol was implemented including 3D T1-weighted structural, diffusion tensor imaging and resting-state functional MR pulse sequences. Following somatotopic segmentation, cortical thickness analyses, probabilistic tractography, BOLD signal analyses and brainstem volumetry were conducted to evaluate cortical, brainstem, structural and functional cortico-medullary and inter-hemispheric connectivity alterations both cross-sectionally and longitudinally.

Results: Our data confirm progressive primary motor cortex degeneration, considerable supplementary- and pre-motor area involvement, progressive brainstem atrophy, cortico-medullary and inter-hemispheric disconnection, and close associations between clinical UMN scores and somatotopic connectivity indices in PLS.

Discussion: PLS is associated with relentlessly progressive motor connectome degeneration. Clinical disability in PLS is likely to stem from a combination of intra- and inter-hemispheric connectivity decline, primary-, pre-, and supplementary motor cortex degeneration. Simple “bedside” clinical tools, such as tapping rates, are excellent proxies of the integrity of the relevant fibres of the contralateral corticospinal tract.

Glossary

AD: axial diffusivity, **ALS**: amyotrophic lateral sclerosis, **ALSFRS-r**: revised amyotrophic lateral sclerosis functional rating scale, **ANOVA**: analysis of variance, **AUC**: area under the curve, **BA**: "bulbar asymptomatic"- patients with spinal onset disease without bulbar manifestations, **BrS**: Brainstem shape, **BOLD**: blood-oxygen-level-dependent (BOLD) signal, **BS**: "bulbar symptomatic"- patients with bulbar symptoms, **Bul**: bulbar segment of the primary motor cortex**,** ***C9orf72***: chromosome 9 open reading frame 72, **CBT**: corticobulbar tract, **CST**: corticospinal tract, **CT**: cortical thickness, **DTI**: diffusion tensor imaging**, DWI**: diffusion weighted imaging, **EMM**: estimated marginal mean, **ELQ**: emotional lability questionnaire, **EPI**: echo-planar imaging, **FA**: fractional anisotropy, **FC**: functional connectivity, **FLAIR**: fluid-attenuated inversion recovery, **fMRI**: functional MRI, **FOV**: field of view, **FSL**: FMRIB´s Software Library, **FTD**: frontotemporal dementia, **FWE**: familywise error, **GM**: grey matter, **HARDI**: high angular resolution diffusion-weighted imaging, **HC**: healthy control, **IR-SPGR**: inversion recovery prepared spoiled gradient recalled echo, **IQR**: interquartile range, **IR-TSE**: inversion recovery turbo spin echo sequence, **LH**: left hemisphere, **LL**: lower limb, **LMN**: lower motor neuron, **Lt**: Left, **M1**: primary motor cortex**, ML**: machine-learning, **MND**: Motor neuron disease, **MNI152**: Montreal Neurological Institute 152 standard space, **MRS**: magnetic resonance spectroscopy, **MV**: medullary volume, **NODDI**: neurite orientation dispersion and density imaging, **PBA**: pseudobulbar affect, **PCC**: pathological crying and laughing, **PLS**: Primary lateral sclerosis, **PM**: premotor area, **PMC**: primary motor cortex, **PUMS**: Penn Upper Motor Neuron Score, **QC**: quality control, **RH**: right hemisphere, **RD**: Radial diffusivity, **ROI**: region of interest, **rsFMRI**: resting-state functional MRI, **Rt**: right, **SBMA**: spinal-bulbar muscular atrophy, **SC**: structural connectivity, **SD**: standard deviation, **SE-EPI**: spin-echo echo planar imaging, **SENSE**: sensitivity Encoding, **SMA**: supplementary motor area, **SPIR**: spectral presaturation with inversion recovery, **T**: Tesla, **T1w**: T1-weighted imaging, **TAP20**: number of taps in 20sec, **TE**: echo time, **TI**: inversion time, **TIV**: total intracranial volume, **TR**: repetition time, **Tukey HSD test**: Tukey's Honest Significant Difference test, **UL**: upper limb, **UMN**: upper motor neuron, **WM**: white matter

Introduction

Primary lateral sclerosis (PLS) is a low-incidence motor neuron disorder with distinctive clinical features. While the natural history and epidemiology of amyotrophic lateral sclerosis is very well characterised, disease propagation in PLS is less well understood, imaging studies are relatively scarce and post mortem studies often include a relatively small number of patients. Compared to ALS, PLS is associated with a better prognosis, and there is a prevailing assumption of slower disease progression based on clinical observations [1, 2]. As there is a paucity of longitudinal neuroimaging studies in PLS, patterns of disease propagation are relatively poorly characterised and it is unclear which imaging markers are optimal for tracking cerebral disease burden. A large number of insightful cross-sectional imaging studies have been published using structural, diffusion, functional and metabolic modalities [3-14] invariably capturing considerably primary motor cortex (PMC), corticospinal tract (CST) and corpus callosum (CC) degeneration. The PMC is typically evaluated as a single region in PLS, overlooking the predilection of symptoms to specific body regions and the likely somatotopic distribution of disease burden within the PMC. Similarly, the CST is also invariably assessed as a single tract, despite its connectivity to specific cortical regions along the motor strip. Disability in PLS is often exclusively linked to PMC and CST degeneration and with few exceptions [3] inter-hemispheric connectivity alterations are under evaluated.

Clinico-radiological correlations in other motor neuron diseases, such as ALS and SBMA are confounded by varying degree of lower motor neuron involvement and often there is a marked disparity between radiological findings and clinical disability [15, 16]. As anterior horn pathology is limited or absent in PLS [17], it is an ideal condition to study clinco-radiological associations offering a rare opportunity to radiologically validate commonly used clinical instruments and cement their role in future pharmacological trials [1, 18].

Currently, there are no effective disease-modifying therapies in PLS, and despite the relatively better prognosis compared to ALS, the condition has very significant quality-of-life implications. Advances in PLS neuroimaging have been previously reviewed and a multitude of methodological approaches have been explored spanning from PET, SPECT, MRS, DTI, and a variety of structural modalities [9, 19]. The relevance of conducting large multimodal academic imaging studies is that a large panel of derived metrics can be systematically interrogated and their respective detection sensitivity and tracking potential can be juxtaposed. The practical utility of imaging markers can then be systematically appraised so that streamlined protocols can be developed for clinical and multi-site pharmacological trial applications [12]. With increasing disability, patients are less likely to tolerate long imaging protocols therefore it is indispensable to establish the priority of pulse-sequences based on their biomarker utility.

Accordingly, the objective of this study is the comprehensive longitudinal analysis of motor network degeneration in PLS, using somatotopic segmentations, and body region-based connectivity analyses. Additionally, we investigate pre- and supplementary motor area involvement and contrast the sensitivity and practical utility of structural and functional connectivity metrics. Our objectives are to determine if progressive radiological changes can be detected in PLS, to verify if the interrogation of resting-state fMRI data provides additional insights, and explore the radiological correlates of routinely used clinical instruments.

Methods

Standard Protocol Approvals, Registrations, and Patient Consents

All participants gave informed consent in accordance with the Ethics Approval of this research study (Beaumont Hospital, Dublin, Ireland - IRB).

Participants and neuroimaging

Neuroimaging data from 41 PLS patients and 108 healthy controls (HC) were included, and a follow-up interval of four months was used for multi-timepoint longitudinal follow-up (**Table 1**). All patients had "definite PLS" according to the recently revised diagnostic criteria [20] Exclusion criteria included prior neurosurgery, previous cerebrovascular events, traumatic brain injury, comorbid neoplastic or neuroinflammatory diagnoses, comorbid psychiatric disease, and inability to tolerate MR scanning. Demographic and clinical variables were carefully recorded on the day of the scan including age, sex, handedness, medications, body region of symptom onset, family history of MND or FTD, medications, Penn Upper Motor Neuron Scale (PUMS) and its subscores, tapping rates in each extremity, and a subset of patients (n=14) were also assessed for the presence of mirror movements. The Penn UMN burden score is a composite measure of pathologically-increased reflexes in each extremity and the bulbar region, and limb spasticity measured on the modified-Ashworth scale. The number of finger and foot taps was measured over 20 seconds with 3 repetitions in each limb and the mean of the number of taps during the three trials was recorded for limb left and right. The neuropsychological profile of patients was evaluated using the Edinburgh Cognitive and Behavioural ALS Screen (ECAS), and performance was interpreted on validated population-based normative values to detect language, verbal fluency, executive, memory and visuospatial impairments. [21] Additionally, the Hospital Anxiety and Depression Scale (HADS), the Frontal Systems Behavior Scale and the Emotional Lability Questionnaire (ELQ) [22] was administered to screen for pseudobulbar affect. Exome sequencing was performed in 32 imaged PLS patients and samples screened for putative variants in the exons and splice sites of 33 genes linked to ALS [23] and 70 genes linked to HSP in the literature [24]. Samples were also screened for GGGGCC hexanucleotide repeat expansion in *C9orf72* using repeat-primed polymerase chain reaction (PCR) as described previously [25].

Neuroimaging

All MR data were acquired on the same 3 Tesla Philips Achieva scanner. Structural data were acquired using a high-resolution T1-weighted (T1w) 3D Inversion Recovery Prepared Spoiled Gradient Recalled Echo (IP-SPGR) pulse sequence, diffusion-weighted data were acquired using a spin-echo EPI sequence, and echo-planar imaging (EPI) sequence was used to evaluate blood oxygen level dependent (BOLD) signal fluctuations with the following parameters: 30 axial slices, repetition time (TR) / echo time (TE) = 2000 ms / 35 ms, flip angle (FA) = 90°, pixel bandwidth = 1780, Hz/Px. T1w and DWI parameters have been previously described [26]; briefly, T1w were acquired with TR/TE = 8.5/3.9 ms, TI =1060 ms, FOV: 256 x 256 x 160 mm, and a spatial resolution: 1 mm^3. 32-direction DTI images were recorded in a FOV = 245 x 245 x 150 mm, with a spatial resolution = 2.5 mm^3, and TR/TE = 7639 / 59 ms. A large panel of radiological indices pertaining to motor function

were systematically evaluated. Morphometric changes were investigated in cortical motor areas using cortical thickness (CT) measurements and in the medulla by volumetry. To assess the entire motor cortex, CT changes were evaluated in the primary motor cortex (PMC), premotor (PM) and supplementary motor area (SMA) using the relevant labels of the HMAT atlas [27]. The Brainnetome atlas was used to define the relevant functional segments of the motor cortex [28]. Both structural and functional cortex-to-medulla and PMC-to-PMC connectivity changes were explored. In each hemisphere, the integrity of three tracts was evaluated connecting the bulbar, upper and lower limb segments of the PMC with the medulla. Inter-hemispheric connectivity was evaluated separately between the contralateral PMCs.

Cortical thickness measurement and medullary volume estimates

Structural T1w data were pre-processed to extract two neuroimaging metrics, medullary volumes and the CT of five ROIs in each hemisphere: (1) "bulbar PMC", (2) "upper limb PMC", (3) "lower limb PMC", (4) premotor (PM), (5) supplementary motor area (SMA). Medullary volumes were derived from FreeSurfer tools, using the "segmentBS" pipeline which segments the medulla based on Bayesian statistics [29]. CT was extracted from FreeSurfer's surface map estimating cortical thickness at each vertex. Data from all vertices comprising the given ROIs was averaged to generate a single CT value for each ROI in each subject. As surface labels are not available for the HMAT atlas, volumetric labels were mapped to the surface using Workbench tools [30]. Additionally, raw T1w data were also pre-processed with FMRIB´s Software Library (FSL) pipelines to generate outputs for downstream image co-registration and normalisation to the MNI152mm space.

Functional connectivity estimation

To estimate functional connectivity (FC), data were first pre-processed in FSL utilising the FEAT pipeline. Brain extraction, slice-time correction, motion correction and correction of head-motion-related artifacts were implemented, the latter using FSL's AROMA algorithm [31]. Each patient's pre-processed functional image was linearly co-registered to the native high-resolution structural image using 6 degrees of freedom (DOFs), and – for higher-level group comparisons – non-linearly warped to the MNI152 2mm standard space with 12 DOFs. FC was defined as the Fisher z-transformed correlation between the mean time courses of the brainstem and the relevant cortical ROI, separately in the two hemispheres. FC was calculated in Matlab R2021b (The Mathworks, Natick, USA), using the CoSMoMVPA [32] and Fieldtrip [33] toolboxes.

Structural connectivity estimation

Structural connectivity (SC) was evaluated based on diffusion-weighted (DW) data. The data were pre-processed using MRtrix3 tools, including noise filtering [34], Gibb's Ringing artifacts removal [35], motion & eddy current correction [36] and bias field correction [37]. DW images were aligned to the high-resolution T1w data and tractograms were calculated between each pair of ROIs using a probabilistic algorithm, producing 5000 streamlines per tract [38]. A more detailed description of our

tractography approach has been previously reported [39]. SC was defined by several metrics associated with white matter microstructure, including axial diffusivity (AD), fractional anisotropy (FA) and radial diffusivity (RD), averaged across each (binarised) tract. These were estimated based on a tensor image fitted to the data by means of weighted least squares estimation.

Statistical modelling

Statistical analyses were conducted in RStudio (R version 4.2.1). Differences in age and education between patients and controls were compared using Welch two-sample t-tests, whereas Chi-square testing was used to compare sex and handedness ratio distributions. Group differences in neuroimaging metrics were explored both cross-sectionally and longitudinally using linear models, accounting for age, sex and handedness; volumetric contrasts were also corrected for total intracranial volumes (TIV). For the cross-sectional analysis, the main effect of group membership ("PLS") was explored and longitudinal patterns were explored in mixed effects models with the fixed effect "Subject" and the random effect "Time" using then nmle package of RStudio. This allows missing data modelling as not all subjects had follow-up data (**Table 1**). Since our objective was to explore progression differences between study groups, the interaction effect Group ("PLS") x Time was evaluated. Finally, associations between neuroimaging metrics and clinical scores were assessed. For the majority of PLS patients (n=40), PUMS sub-scores lateralised to left and right and for upper and lower extremities separately as well as tapping rates were available at one of the MR scanning session. We have therefore explored associations between clinical scores and neuroimaging using a linear model, correcting for age, sex and handedness. We limited our analysis on physiological functional associations, i.e. lateralised clinical scores with contralateral cerebral neuroimaging metrics. Only for non-lateralised bulbar PUMS scores were averaged bilateral neuroimaging metrics from both hemispheres utilised. The alpha level for all explorations was set to $p < 0.05$.

Data availability

Group-level outputs, statistical maps, variable distributions, post-hoc statistics and additional information on data processing pipelines can be requested from the corresponding author. Individual patient clinical and neuroimaging data cannot be made available due to institutional regulations and departmental policies.

Results

Demographics

The demographic profile and statistical comparisons between study groups are presented in **Table 1**. The groups were adequately matched for age ($t(76.40) = 1.58$, $p = 0.12$), sex (X^2 (1, N = 149) = 1.03, $p = 0.31$) and handedness (X^2 (1, N = 149) = 0.11, $p = 0.74$), but PLS patients had significantly less years of education ($t(77.70) = -3.75$, $p < 0.001$). Irrespective of group differences these variables were included as covariates in the statistical models. The patients tested negative for genetic variants associated with ALS and HSP as well as GGGGCC hexanucleotide repeat expansions. Five out of 14 patients exhibited mirror movements.

Neuroimaging metrics

Statistical outcomes of neuroimaging contrasts are summarised in **Table 2** and illustrated in **Figures 1–4. Figures 5 and 6** depict the associations between neuroimaging metrics and clinical scores and **Supplementary Table 1** provides additional statistical details.

Medullary volume and motor cortex cortical thickness differentiate PLS patients from controls both at baseline and in progression

Both medullary volume and motor cortex thickness differentiate PLS from HC, both cross-sectionally and longitudinally (**Figure 1**). PLS patients exhibit lower medullary volumes at baseline [$t(144) = -3.72$, $p < 0.001$] and exhibit faster rates of volume loss [$t(117) = -2.43$, $p = 0.017$]. Cortical thickness of all motor cortex ROIs (bulbar PMC, upper limb PMC, lower limb PMC, PM, SMA) was significantly thinner at baseline in both hemispheres. **Figure 2** illustrates these findings in the left-hemisphere and Table 2 provides comprehensive descriptive statistics. Moreover, in a subset of the ROIs, cortical thinning over time was more rapid in PLS; RH: bulbar ROI ($t(117) = -2.41$, $p = 0.018$), lower limb ROI ($t(117) = -2.22$, $p = 0.028$; LH: bulbar ROI ($t(117) = -2.66$, $p = 0.009$), upper limb ROI ($t(117) = -2.66$, $p = 0.009$), PM ($t(117) = -2.43$, $p = 0.017$)]. **Table 2** presents the relevant statistical comparisons.

Inter-hemispheric disconnection between the motor cortices in PLS

Radiological evidence was identified for inter-hemispheric disconnection in PLS between the two motor cortices (**Figure 3**) as demonstrated by decreased FA [($t(144) = -2.69$, $p = 0.008$] and increased RD [($t(144) = 2.59$, $p = 0.011$] between the left and right M1. We did not detect inter-hemispheric functional PMC disconnection and no progressive changes were detected either. Output statistics are provided in **Table 2**.

Cortico-medullary disconnection

Our multimodal imaging data confirms reduced motor cortex - medulla connectivity in patients with PLS (**Figure 4**). This is evidenced by decreased FA in PLS patients at baseline in both hemispheres for the majority of relevant tracts [RH: bulbar tract ($t(144) = -2.18$, $p = 0.031$), lower limb tract ($t(144) = -3.43.$, $p < 0.001$), upper limb tract ($t(144) = -2.50$, $p = 0.014$); LH: upper limb tract ($t(144) = -2.98$, $p =$

0.003), lower limb tract (t(144) = -2.91, p = 0.004)]. PM (t(144) = -2.43, p = 0.017)]. A tendency for reduced functional connectivity was also detected in both hemispheres between the bulbar ROIs and medulla [RH: t(144) = -1.79, p = 0.075; LH: t(144) = -1.72, p = 0.088]. No progressive connectivity decline was ascertained within the longitudinal follow-up interval of this cohort. Table 2 summarises the relevant statistical outputs.

Associations between neuroimaging metrics are clinical scores

PUMS scores are closely associated with anatomically relevant connectivity markers (**Figure 5, Supplementary Table 1**.): higher bulbar PUMS scores, i.e. worse disability, correlated with lower FA [t(19) = -2.78, p = 0.009], and higher RD [t(19) = 2.58, p = 0.015] in the corticobulbar tracts. Higher left arm PUMS scores correlated with lower FA [t(19) = -2.60, p = 0.014], higher AD [t(19) = 2.67, p = 0.012], and higher RD [t(19) = 3.37, p = 0.002] in the right-hemispheric "arm-CST". Similarly, higher right arm PUMS scores correlated with higher left-hemispheric AD [t(19) = 3.05, p = 0.005] and higher RD [t(19) = 2.26, p = 0.031]. Left leg PUMS scores correlated with higher RD [t(19) = 2.05, p = 0.049], and a tendency for higher AD [t(19) = 1.93, p = 0.063] was also detected in the right "leg-CST" i.e. the tract linking the leg-segment of the motor homunculus to the medulla. No significant associations were detected between the right lower limb PUMS scores and the relevant tracts, but a trend of association was identified between higher scores and higher RD [t(19) = 1.77, p = 0.087] and lower FC [t(19) = -1.73, p = 0.100].

Tapping rates also showed close associations with structural connectivity metrics (**Figure 6, Supplementary Table 1**). Lower left upper limb tapping rates correlate with lower right-hemispheric "arm-CST" FA [t(19) = 2.62, p = 0.014] and higher RD [t(19) = -2.65, p = 0.013]. Lower right hand tapping rates are associated with higher left-hemispheric "arm-CST" RD [t(19) = -2.45, p = 0.021]. Lower left foot limb tapping rates are associated with lower right-hemispheric "leg-CST" FA [t(19) = 2.21, p = 0.036] and higher RD [t(19) = -2.24, p = 0.033]. Not direct associations were detected between right lower limb tapping rates and contralateral structural connectivity, but a trend was identified for an association between lower right foot tapping rates and lower left-hemispheric FC and [t(19) = 1.68, p = 0.109]. Interestingly, no direct associations were detected between CT and PUMS score or tapping rates.

Discussion

In addition to confirming progressive primary motor cortex degeneration, our results also demonstrate considerable supplementary- and pre-motor involvement, progressive brainstem atrophy, cortico-medullary and inter-hemispheric disconnection, and close associations between clinical UMN scores and somatotopic connectivity indices.

Motor disability in PLS is typically exclusively linked to primary motor cortex degeneration, but our analyses demonstrate additional pre- and supplementary- motor area pathology which are likely to contribute to motor disability. The premotor area is classically implicated in movement planning, the preparation of postural muscles for forthcoming movements, spatial guidance of movement, and in the sensory guidance of movements. SMA is thought to contribute to postural stability, movement initiation, coordination of temporal sequences of actions, and bimanual coordination. Similar to ALS, extrapyramidal dysfunction is also likely to significantly contribute to motor disability in PLS [40-43]. Previous PLS studies have invariably evaluated the primary motor cortex as a single cortical region without its somatotopic segmentation. Similarly, previous PLS studies evaluate the corticospinal tract as a single tract, without parcellation into sub-tracts originating from the lower limb, upper limb and bulbar segments of the motor cortex. The segmentation of the PMC and CST into functionally defined, somatotopic sub-regions permits a more nuanced characterisation of motor connectome degeneration. In turn, the interrogation of the integrity metrics of these labels allows more direct associations with regional UMN metrics. In other MNDs, such as ALS, direct clinico-radiological correlations between disability scores and cerebral measures are widely considered contentious [15] as motor disability stems from a combination of upper- and lower motor neuron pathology often disproportionately driven by LMN dysfunction. PLS is an ideal phenotype to explore associations between brain metrics and clinical measures which in turn permits both the validation of clinical instruments as well as highlighting the value of MRI-derived indices [18, 44].

The clinico-radiological correlations of this study corroborate the validity and utility of cheap, easily-administered clinical tests, both established instruments (PUMNS) as well as simple quantitative tools such as tapping rates. Tapping rates exhibit excellent concordance with contralateral CST metrics both in the upper- and lower limb segments. These associations suggest that disability is closely related to motor connectome disintegration and suggest that these clinical tests could be readily used for both monitoring purposes as well as potential endpoints in clinical trials. The lack of direct associations between cortical thickness measures and clinical UMN signs confirms the value of connectivity metrics. It also highlights that clinical disability should not be linked to focal cortical measures alone, but symptoms stem from the disconnection of physiologically interconnected brain regions, in this case, the close interplay between the brainstem, motor cortex, pre- and supplementary motor regions.

Our findings reveal that disability in PLS is primarily driven by somatotopic degeneration of the motor system, and PLS is not solely associated with intra-hemispheric but also inter-hemispheric degeneration disconnection. While the evaluation of FA is sometimes criticised as a mere composite measure of white matter integrity, it has captured baseline connectivity changes where AD and RD did not detect significant alterations. RD was also affected in the inter-hemispheric callosal fibres connecting the contralateral motor cortices. Despite the limited RD and AD changes in our comparative analyses where PLS patients were contrasted to controls, these measures showed

excellent correlation with clinical metrics highlighting the importance of evaluating a large panel of white matter metrics rather than FA alone.

The relatively limited longitudinal change in connectivity metrics over the 16 month follow-up suggest that considerable change may have already taken place at study entry and that rate of progression after diagnosis may be relatively slow; this is sometimes referred to as ceiling- or flooring-effect of a given variable. These metrics may have a good utility in differentiating patients from controls, but limited in tracking patients over time. Conversely, medullary volumes and cortical thickness values in the bulbar segment of the motor cortex and the premotor area continue to decline over time, making them better suited for monitoring markers. From a biomarker perspective, no single imaging marker can address both the diagnostic and monitoring requirements of PLS and therefore, a panel of several metrics with complementary detection profiles are required. One of the practical deliverables of academic imaging studies is the appraisal of a large panel of imaging measures with regards to their clinical utility so that streamlined, short-duration protocols can be developed for the pragmatic needs of clinical and pharmacological trial applications. Accordingly, our observations may have implications for the design of clinical protocols. While changes in fMRI connectivity metrics are largely consistent with diffusivity-derived structural connectivity alterations, they are less significant and add relatively little additional information. This is further demonstrated by our inter-hemispheric analyses where FA, AD, RD readily capture the disconnection between the two PMCs whereas fMRI fails to detect this. It is also noteworthy that raw fMRI data typically has a much lower spatial resolution than DTI data, and pre-processing and subsequent data analyses are also often more complex [45]. Furthermore, the impact of underlying vascular and pharmacological factors, such as hypertension, smoking, diabetes, and medications such as TCAs, SSRIS, benzodiazepines and central acting anti-spasticity medications on BOLD signal are not fully elucidated and may be important confounders. Accordingly, our data suggest that in clinical applications, a high-resolution 3D T1-weighted pulse sequence and a DTI sequence offers ample metrics to quantitatively assess grey and white matter integrity and the practical biomarker value of routine rs-fMRI acquisition may be relatively limited. Other imaging modalities, such as high angular resolution diffusion-weighted imaging (HARDI), neurite orientation dispersion and density imaging (NODDI) or magnetic resonance spectroscopy (MRS) are complementary techniques which have generated important insights in other motor neuron diseases [46]. The additional relevance of evaluating a large panel of metrics is gauging their potential as features in future machine-learning (ML) applications. ML models are increasingly applied to MND data sets and a variety of mathematic models have been recently explored [47, 48].

This paper is not without limitations, mirror movements were only evaluated in 14 patients and genetic information is only available in 32 patients. fMRI analyses are limited to resting-state data as no motor paradigms were utilised in this study. All of the participants had “definite” PLS based on the recent consensus criteria consistent with their relatively long symptom duration. The inclusion of additional patients with “probable” PLS may have generated additional insights with regards to the earlier phases of PLS [49, 50]. Notwithstanding these limitations, our paper demonstrates progressive motor connectome disconnection in PLS, significant inter-hemispheric connectivity alterations, somatotopic involvement of cortical regions and descending corticospinal tracts. The considerable association with simple, cheap and readily administered clinical metrics highlight the utility of these instruments in everyday clinical practice.

Conclusions

PLS is associated with both intra- and inter-hemispheric connectivity reductions. Simple clinical instruments, such as UMN scores and taping rates readily correlate with MRI-derived pyramidal tract measures confirming their utility in assessing disease burden non-invasively.

Acknowledgements

We are most grateful for the participation of each patient and healthy control, and we also thank all patients who expressed interest in this research study but were unable to participate for medical or logistical reasons. We also express our gratitude to the caregivers of PLS patients for facilitating attendance at our neuroimaging centre. Without their generosity this study would have not been possible.

Funding information

This study was sponsored by the Spastic Paraplegia Foundation (SPF). Professor Bede is also supported by the Health Research Board (HRB EIA-2017-019 & JPND-Cofund-2-2019-1), the Irish Institute of Clinical Neuroscience (IICN), the EU Joint Programme – Neurodegenerative Disease Research (JPND), the Andrew Lydon scholarship, and the Iris O'Brien Foundation. RLMcL, MAD and JCH are supported by the MND Association (898-792) and Science Foundation Ireland (17/CDA/4737).

Conflicts of interest disclosure

The authors have no conflicts of interests to declare.

Authorship contribution

The manuscript was drafted by MT, ELT, WFS, PB. Study conceptualisation: MT, EF, PB. Clinical assessments: EF, SLHS, RC, OH, PB. MR data processing and analyses: MT, ELT, PB. Genetics analyses: RLMcL, MAD, JCH. The manuscript was reviewed for intellectual content by RC, JCH, OH, MAD, RLMcL.

Ethics approval

This study was approved by the Ethics (Medical Research) Committee—Beaumont Hospital, Dublin, Ireland (IRB).

Data Availability Statement

The data that support the findings of this study are available on request from the corresponding author. The data are not publicly available due to privacy or ethical restrictions.

Table 1. Demographic and clinical details

	PLS	**HC**	***Welch two-sample t-test [W] or Chi-squared [C2]***
Total number of subjects (missing T1/DWI/fMRI at baseline)	41 (1/2/3)	108 (0/1/0)	*n.a.*
Age [y, mean ± SD]	62.00 ± 10.09	59.02 ± 10.72	*W:* $t(76.40) = 1.58$, $p = 0.12$
Sex, F/M	16/25	54/54	*C2:* $X^2(1, N = 149) = 1.03$, $p = 0.31$
Handedness, R/L	37/4	101/7	*C2:* $X^2(1, N = 149) = 0.11$, $p = 0.74$
Baseline scans [count]	41	108	*n.a.*
4-month follow-up [count]	30	18	*n.a.*
8-month follow-up [count]	25	13	*n.a.*
12-month follow-up [count]	19	8	*n.a.*
16-month follow-up [count]	7	0	*n.a.*
Mirror movements [N=14]	5	*n.a*	*n.a*
Penn UMN32-score ± SD (last MRI session)	21.12 ± 6.40	*n.a.*	*n.a.*
Penn bulbar subscore ± SD (last MRI session)	2.00 ± 1.40	*n.a.*	*n.a.*
Penn R_UL subscore ± SD (last MRI session)	4.32 ± 1.70	*n.a.*	*n.a.*
Penn L_UL subscore ± SD (last MRI session)	4.41 ± 1.60	*n.a.*	*n.a.*
Penn R_LL subscore ± SD (last MRI session)	5.32 ± 1.46	*n.a.*	*n.a.*
Penn L_LL subscore ± SD (last MRI session)	5.07 ± 1.46	*n.a.*	*n.a.*
TAP20 R_UL mean ± SD (last MRI session) *[N=38]*	50.33 ± 22.30	*n.a.*	*n.a.*
TAP20 L_UL mean ± SD (last MRI session) *[N=38]*	45.34 ± 19.66	*n.a.*	*n.a.*
TAP20 R_LL mean ± SD (last MRI session) *[N=38]*	26.49 ± 11.70	*n.a.*	*n.a.*
TAP20 L_LL mean ± SD (last MRI session) *[N=38]*	25.38 ± 13.89	*n.a.*	*n.a.*
Cognitive impairment on ECAS	9 (21.9%)	*n.a*	*n.a*
ELQ-Laughing [N=40] mean Abnormal	5.6 31%	*n.a.*	*n.a.*
ELQ-Crying [N=40] mean abnormal	4.0 25%	*n.a.*	*n.a.*

Abbreviations: ELQ = emotional lability questionnaire, F = female, HC = healthy control, L = left-handed, L_LL = left lower limb, L_UL = left upper limb, M = male, MRI = magnetic resonance imaging, N = sample size, n.a. = not applicable, Penn = Penn Upper Motor Neuron Score, PLS = primary lateral sclerosis, R = right-handed, R_LL = right lower limb, R_UL = right upper limb, s = seconds, SD = standard deviation, TAP20 = average number of taps in 20sec (mean), y = years, * = significant at an alpha-level of $p<=0.05$

Table 2. Statistical comparisons of neuroimaging metrics between patients with PLS and healthy controls.

	Cross-sectional (Main effect: *Group "PLS"*)						**Longitudinal (Interaction: *Group "PLS" x Time*)**					
	Right hemisphere			Left hemisphere			Right hemisphere			Left hemisphere		
	Esti-mate	*t*-value	*p*-value	esti-mate	*t* -value	*p*-value	esti-mate	*t*-value	*p*-value	esti-mate	*t*-value	*p*-value
Medulla volume												
Vol	-2.58e-4	-3.72	**<.001***	*n.a.*	*n.a.*	*n.a.*	-6.23e-5	-2.43	**0.017***	*n.a.*	*n.a.*	*n.a.*
Cortical thickness												
Bul	-0.162	-4.64	**<.001***	-0.129	-4.08	**<.001***	-0.081	-2.41	**0.018***	-0.080	-2.66	**0.009***
UL	-0.241	-7.07	**<.001***	-0.221	-6.16	**<.001***	-0.038	-1.22	0.225	-0.066	-2.66	**0.009***
LL	-0.185	-4.78	**<.001***	-0.274	-6.40	**<.001***	-0.052	-1.87	**0.064+**	-0.028	-0.977	0.331
PM	-0.160	-6.21	**<.001***	-0.164	-6.75	**<.001***	-0.058	-2.22	**0.028***	-0.062	-2.43	**0.017***
SMA	-0.164	-5.27	**<.001***	-0.247	-7.58	**<.001***	-0.044	-1.55	0.124	-0.019	-0.670	0.504
Bulbar-cortex to medulla connectivity												
AD	-7.98e-6	-0.249	0.804	1.36e-5	0.328	0.743	-2.88e-6	-0.081	0.935	-9.81e-6	-0.291	0.772
FA	-0.029	-2.18	**0.031***	-0.025	-1.45	0.149	-0.005	-0.411	0.682	-0.010	-0.778	0.439
RD	1.24e-5	0.792	0.430	2.96e-5	1.51	0.133	4.20e-6	0.242	0.809	3.24e-6	0.211	0.834
FC	-0.114	-1.79	**0.075+**	-0.068	-1.72	**0.088+**	-0.037	-1.40	0.165	-0.002	-0.080	0.936
Upper-limb-cortex to medulla connectivity												
AD	-3.79e-5	-1.04	0.302	-6.66e-6	-0.205	0.838	1.56e-5	0.456	0.649	5.99e-6	-0.178	0.859
FA	-0.049	-3.43	**0.001***	-0.038	-2.98	**0.003***	0.003	0.245	0.807	-0.002	-0.207	0.836
RD	7.19e-6	0.403	0.688	2.29e-5	1.42	0.157	7.11e-6	0.469	0.640	5.53e-6	0.338	0.736
FC	0.028	0.841	0.402	0.030	0.871	0.385	-0.010	-0.432	0.667	-0.021	-0.875	0.383
Lower-limb-cortex to medulla connectivity												
AD	-3.19e-6	-0.100	0.921	-6.28e-6	-0.194	0.846	1.08e-6	0.031	0.975	-6.16e-6	-0.174	0.862
FA	-0.032	-2.50	**0.014***	-0.038	-2.91	**0.004***	-0.003	-0.234	0.815	-0.007	-0.583	0.561
RD	1.89e-5	1.20	0.230	2.28e-5	1.42	0.158	3.10e-6	0.188	0.852	1.17e-6	0.074	0.942
FC	0.019	0.617	0.538	0.0513	1.60	0.113	-0.014	-0.662	0.5091	-0.019	-0.800	0.426
Inter-PMC connectivity												
AD	2.69e-5	0.737	0.462	*n.a.*	*n.a.*	*n.a.*	-7.71e-6	-0.227	0.821	*n.a.*	*n.a.*	*n.a.*
FA	-0.035	-2.69	**0.008***	*n.a.*	*n.a.*	*n.a.*	-0.007	-0.695	0.489	*n.a.*	*n.a.*	*n.a.*
RD	5.05e-5	2.59	**0.011***	*n.a.*	*n.a.*	*n.a.*	4.16e-7	0.025	0.980	*n.a.*	*n.a.*	*n.a.*
FC	-0.040	-0.893	0.374	*n.a.*	*n.a.*	*n.a.*	0.009	0.262	0.794	*n.a.*	*n.a.*	*n.a.*

Bilateral metrics are presented in under the relevant hemisphere; metrics from single structures such as medullary volumes and inter-hemispheric connectivity metrics are presented in the "Right hemisphere" columns.

Abbreviations: AD = axial diffusivity, Bul = bulbar, CT = cortical thickness, FA = fractional anisotropy, FC = functional connectivity, HC = healthy control, LL = lower limb, PMC = primary motor cortex, MRI = magnetic resonance imaging, *n.a.* = not applicable, PM = premotor cortex, RD = radial diffusivity, SMA = supplementary motor area, TAP = tapping, UL = upper limb, Vol = volumetry (of the medulla), * = significant at an alpha-level of $p \leq 0.05$, $^{+}$ = approaching significance at an alpha-level of $p \leq 0.10$

Figure legends

Figure 1. The medulla was segmented individually for each subject (A) to compare medullary volumes (MV) between patients with PLS controls cross-sectionally (B) and longitudinally (C); lower MV is observed in PLS at baseline (B) with a more rapid volume loss over time (C). Statistical details are provided in table 2. Boxplots represent medians ±1 quartile; whiskers denote data range spanning median ±1.58 ×IQR√n; dots represent outliers; IQR is the interquartile range. Longitudinal comparisons (C) are illustrated as linear models and the respective 95% confidence interval is presented by grey shading. * denotes statistical significance of unpaired t-tests, thresholded at $p \leq 0.05$. **HC**: healthy controls, **PLS**: patients with primary lateral sclerosis, **MV**: medullary volume

Figure 2. Cortical thickness (CT) of five distinct motor cortical ROIs was extracted in each hemisphere (A). At baseline (B), PLS patients exhibited reduced CT in each ROI in both hemispheres compared to controls. Similarly, the progression of cortical thinning was more rapid in PLS compared to controls in most ROIs including Bul, UL, and PM in the left hemisphere; and Bul, PM in the right hemisphere. This figure only illustrates left-hemispheric CT outcomes but table 2 provides the comprehensive statistics for both hemispheres. Boxplots (middle column) represent medians ±1 quartile; whiskers denote the data range spanning median ±1.58 ×IQR√n; dots represent outliers; and IQR is the interquartile range. Longitudinal comparisons (right column) are illustrated as linear models (coloured lines) and the respective 95% confidence interval shown in grey shading. * denotes statistical significance of unpaired t-tests, thresholded at $p \leq 0.05$. **Bul**: bulbar cortex, **CT**: cortical thickness, **HC**: healthy controls, **PLS**: patients with primary lateral sclerosis, **PM**: premotor cortex, **LH**: left hemisphere, **LL**: lower limb, **RH**: right hemisphere, **ROI**: region of interest, **SMA**: supplementary motor area, **UL**: upper limb

Figure 3. Inter-hemispheric structural (SC) and functional connectivity (FC) alterations between the contralateral primary motor cortices (A) were evaluated in patients with PLS in contrasts to healthy controls. Inter-hemispheric disconnection is suggested by significantly lower FA (B, first row) and significantly higher RD (B, second row) in PLS at baseline. No baseline AD or FC differences were identified and no longitudinal differences over time (C). Table 2 provides comprehensive statistical details. Boxplots (middle column) represent medians ±1 quartile; whiskers denote data range spanning median ±1.58 ×IQR√n; dots represent outliers; IQR is the interquartile range. Longitudinal comparisons (right column) are illustrated as linear models (coloured lines) and their respective 95% confidence interval shown in grey shading. * denotes statistical significance of unpaired t-tests, thresholded at $p \leq 0.05$. **AD**: axial diffusivity, **FA**: fractional anisotropy, **FC**: functional connectivity, **HC**: healthy controls, **PLS**: patients with primary lateral sclerosis, **RD**: radial diffusivity, **SC**: structural connectivity

Figure 4. Alterations in structural crotico-medullary connectivity in PLS originating from the three functional segments of the motor strip; bulbar, upper- and lower-limb. Lower baseline FA values are detected in all three tracts in the right hemisphere and lower FA identified in the tracts originating from the upper (B) and lower-limb representation in the left hemisphere. Longitudinal progression in FA decline over the study period did not reach significance. Detailed output statistics are provided in **Table 2**. Boxplots (middle column) represent medians ±1 quartile; whiskers denote data range spanning median ±1.58 ×IQR√n; dots represent outliers; IQR is the interquartile range. Longitudinal comparisons (right column) are illustrated as linear models (coloured lines) and their respective 95% confidence interval is shown in grey shading. * denotes statistical significance of unpaired t-tests, thresholded at $p \leq 0.05$. FA: fractional anisotropy, FC: functional connectivity, HC: healthy controls, PLS: patients with primary lateral sclerosis, ROI: region of interest, SC: structural connectivity

Figure 5. Associations between neuroimaging metrics and upper motor neuron symptom burden: Correlations between body-region-specific PUMS sub-scores and anatomically relevant MRI indices. Red boxes highlight statistically significant association at $p \leq 0.05$; grey boxes indicate a tendency for statistical significance ($p \leq .10$). Only lest sided clinical scores are presented for clarity, but **Supplementary Table 1** presents detailed statistical outputs for each subscores left and right. **FA**: fractional anisotropy, **FC**: functional connectivity, **HC**: healthy controls, **PLS**: patients with primary lateral sclerosis, **PUMS**: Penn Upper Motor Neuron Score, **RD**: radial diffusivity, **ROI**: region of interest, **SC**: structural connectivity

Figure 6. Associations between tapping rates and anatomically relevant contralateral neuroimaging metrics. Only the associations between lest sided clinical scores and right hemispheric MRI measures are presented for clarity, but **Supplementary Table 1** provides detailed statistical outputs for each subscores left and right. Red boxes denote statistically significant associations at $p \leq 0.05$, grey boxes indicate a tendency for statistical significance ($p \leq .10$). **FA**: fractional anisotropy, **FC**: functional connectivity, **HC**: healthy controls, **PLS**: patients with primary lateral sclerosis, **PUMS**: Penn Upper Motor Neuron Score, **RD**: radial diffusivity, **ROI**: region of interest, **SC**: structural connectivity

References

[1]. Mitsumoto H, Nagy PL, Gennings C*, et al.* Phenotypic and molecular analyses of primary lateral sclerosis. *Neurol Genet*. 2015;1**:**e3.

[2]. Brugman F, Veldink JH, Franssen H*, et al.* Differentiation of hereditary spastic paraparesis from primary lateral sclerosis in sporadic adult-onset upper motor neuron syndromes. *Arch Neurol*. 2009;66**:**509-514.

[3]. Agosta F, Galantucci S, Riva N*, et al.* Intrahemispheric and interhemispheric structural network abnormalities in PLS and ALS. *Hum Brain Mapp*. 2014;35**:**1710-1722.

[4]. Finegan E, Li Hi Shing S, Chipika RH*, et al.* Widespread subcortical grey matter degeneration in primary lateral sclerosis: a multimodal imaging study with genetic profiling. *Neuroimage Clin*. 2019;24**:**102089.

[5]. Clark MG, Smallwood Shoukry R, Huang CJ, Danielian LE, Bageac D, Floeter MK. Loss of functional connectivity is an early imaging marker in primary lateral sclerosis. *Amyotroph Lateral Scler Frontotemporal Degener*. 2018;19**:**562-569.

[6]. Chipika RH, Christidi F, Finegan E*, et al.* Amygdala pathology in amyotrophic lateral sclerosis and primary lateral sclerosis. *J Neurol Sci*. 2020;417**:**117039.

[7]. Turner MR, Hammers A, Al-Chalabi A*, et al.* Cortical involvement in four cases of primary lateral sclerosis using [(11)C]-flumazenil PET. *J Neurol*. 2007;254**:**1033-1036.

[8]. Agosta F, Canu E, Inuggi A*, et al.* Resting state functional connectivity alterations in primary lateral sclerosis. *Neurobiol Aging*. 2014;35**:**916-925.

[9]. Pioro EP, Turner MR, Bede P. Neuroimaging in primary lateral sclerosis. *Amyotroph Lateral Scler Frontotemporal Degener*. 2020;21**:**18-27.

[10]. Tu S, Menke RAL, Talbot K, Kiernan MC, Turner MR. Cerebellar tract alterations in PLS and ALS. *Amyotroph Lateral Scler Frontotemporal Degener*. 2019;20**:**281-284.

[11]. Iwata NK, Kwan JY, Danielian LE*, et al.* White matter alterations differ in primary lateral sclerosis and amyotrophic lateral sclerosis. *Brain*. 2011;134**:**2642-2655.

[12]. Muller HP, Agosta F, Gorges M*, et al.* Cortico-efferent tract involvement in primary lateral sclerosis and amyotrophic lateral sclerosis: A two-centre tract of interest-based DTI analysis. *Neuroimage Clin*. 2018;20**:**1062-1069.

[13]. Bede P, Murad A, Lope J*, et al.* Phenotypic categorisation of individual subjects with motor neuron disease based on radiological disease burden patterns: A machine-learning approach. *J Neurol Sci*. 2021;432**:**120079.

[14]. Müller HP, Gorges M, Kassubek R, Dorst J, Ludolph AC, Kassubek J. Identical patterns of cortico-efferent tract involvement in primary lateral sclerosis and amyotrophic lateral sclerosis: A tract of interest-based MRI study. *Neuroimage: Clinical*. 2018;18**:**762-769.

[15]. Verstraete E, Turner MR, Grosskreutz J, Filippi M, Benatar M. Mind the gap: the mismatch between clinical and imaging metrics in ALS. *Amyotroph Lateral Scler Frontotemporal Degener*. 2015;16**:**524-529.

[16]. Pradat PF, Bernard E, Corcia P*, et al.* The French national protocol for Kennedy's disease (SBMA): consensus diagnostic and management recommendations. *Orphanet J Rare Dis*. 2020;15**:**90.

[17]. Mackenzie IRA, Briemberg H. TDP-43 pathology in primary lateral sclerosis. *Amyotroph Lateral Scler Frontotemporal Degener*. 2020**:**1-7.

[18]. Mitsumoto H, Chiuzan C, Gilmore M*, et al.* Primary lateral sclerosis (PLS) functional rating scale: PLS-specific clinimetric scale. *Muscle Nerve*. 2020;61**:**163-172.

[19]. Bede P, Pradat PF, Lope J, Vourc'h P, Blasco H, Corcia P. Primary Lateral Sclerosis: Clinical, radiological and molecular features. *Rev Neurol (Paris)*. 2021.

[20]. Turner MR, Barohn RJ, Corcia P*, et al.* Primary lateral sclerosis: consensus diagnostic criteria. *J Neurol Neurosurg Psychiatry*. 2020;91**:**373-377.

[21]. Pinto-Grau M, Burke T, Lonergan K*, et al.* Screening for cognitive dysfunction in ALS: validation of the Edinburgh Cognitive and Behavioural ALS Screen (ECAS) using age and education adjusted normative data. *Amyotroph Lateral Scler Frontotemporal Degener*. 2017;18**:**99-106.

[22]. Newsom-Davis IC, Abrahams S, Goldstein LH, Leigh PN. The emotional lability questionnaire: a new measure of emotional lability in amyotrophic lateral sclerosis. *J Neurol Sci*. 1999;169:22-25.
[23]. Abel O, Shatunov A, Jones AR, Andersen PM, Powell JF, Al-Chalabi A. Development of a Smartphone App for a Genetics Website: The Amyotrophic Lateral Sclerosis Online Genetics Database (ALSoD). *JMIR mHealth and uHealth*. 2013;1:e18-e18.
[24]. Klebe S, Stevanin G, Depienne C. Clinical and genetic heterogeneity in hereditary spastic paraplegias: from SPG1 to SPG72 and still counting. *Rev Neurol (Paris)*. 2015;171:505-530.
[25]. Byrne S, Elamin M, Bede P*, et al.* Cognitive and clinical characteristics of patients with amyotrophic lateral sclerosis carrying a C9orf72 repeat expansion: a population-based cohort study. *Lancet Neurol*. 2012;11:232-240.
[26]. Bede P, Chipika RH, Christidi F*, et al.* Genotype-associated cerebellar profiles in ALS: focal cerebellar pathology and cerebro-cerebellar connectivity alterations. *J Neurol Neurosurg Psychiatry*. 2021;92:1197-1205.
[27]. Mayka MA, Corcos DM, Leurgans SE, Vaillancourt DE. Three-dimensional locations and boundaries of motor and premotor cortices as defined by functional brain imaging: a meta-analysis. *Neuroimage*. 2006;31:1453-1474.
[28]. Fan L, Li H, Zhuo J*, et al.* The Human Brainnetome Atlas: A New Brain Atlas Based on Connectional Architecture. *Cereb Cortex*. 2016;26:3508-3526.
[29]. Iglesias JE, Van Leemput K, Bhatt P*, et al.* Bayesian segmentation of brainstem structures in MRI. *Neuroimage*. 2015;113:184-195.
[30]. Marcus DS, Harwell J, Olsen T*, et al.* Informatics and data mining tools and strategies for the human connectome project. *Front Neuroinform*. 2011;5:4.
[31]. Pruim RHR, Mennes M, van Rooij D, Llera A, Buitelaar JK, Beckmann CF. ICA-AROMA: A robust ICA-based strategy for removing motion artifacts from fMRI data. *Neuroimage*. 2015;112:267-277.
[32]. Oosterhof NN, Connolly AC, Haxby JV. CoSMoMVPA: Multi-Modal Multivariate Pattern Analysis of Neuroimaging Data in Matlab/GNU Octave. *Front Neuroinform*. 2016;10:27.
[33]. Oostenveld R, Fries P, Maris E, Schoffelen JM. FieldTrip: Open source software for advanced analysis of MEG, EEG, and invasive electrophysiological data. *Comput Intell Neurosci*. 2011;2011:156869.
[34]. Veraart J, Fieremans E, Novikov DS. Diffusion MRI noise mapping using random matrix theory. *Magn Reson Med*. 2016;76:1582-1593.
[35]. Kellner E, Dhital B, Kiselev VG, Reisert M. Gibbs-ringing artifact removal based on local subvoxel-shifts. *Magn Reson Med*. 2016;76:1574-1581.
[36]. Smith SM, Jenkinson M, Woolrich MW*, et al.* Advances in functional and structural MR image analysis and implementation as FSL. *Neuroimage*. 2004;23 Suppl 1:S208-219.
[37]. Tustison NJ, Avants BB, Cook PA*, et al.* N4ITK: improved N3 bias correction. *IEEE Trans Med Imaging*. 2010;29:1310-1320.
[38]. Tournier JD, Calamante F, Connelly A. Improved probabilistic streamlines tractography by 2nd order integration over fibre orientation distributions. *Proceedings of the International Society for Magnetic Resonance in Medicine (ISMRM)*. 2010;18.
[39]. Tahedl M, Murad A, Lope J, Hardiman O, Bede P. Evaluation and categorisation of individual patients based on white matter profiles: Single-patient diffusion data interpretation in neurodegeneration. *J Neurol Sci*. 2021;428:117584.
[40]. Feron M, Couillandre A, Mseddi E*, et al.* Extrapyramidal deficits in ALS: a combined biomechanical and neuroimaging study. *J Neurol*. 2018;265:2125-2136.
[41]. Finegan E, Hi Shing SL, Chipika RH*, et al.* Thalamic, hippocampal and basal ganglia pathology in primary lateral sclerosis and amyotrophic lateral sclerosis: Evidence from quantitative imaging data. *Data Brief*. 2020;29:105115.
[42]. Abidi M, de Marco G, Grami F*, et al.* Neural Correlates of Motor Imagery of Gait in Amyotrophic Lateral Sclerosis. *J Magn Reson Imaging*. 2021;53:223-233.

[43]. Abidi M, de Marco G, Couillandre A*, et al.* Adaptive functional reorganization in amyotrophic lateral sclerosis: coexisting degenerative and compensatory changes. *Eur J Neurol*. 2020;27**:**121-128.
[44]. Mitsumoto H, Ulug AM, Pullman SL*, et al.* Quantitative objective markers for upper and lower motor neuron dysfunction in ALS. *Neurology*. 2007;68**:**1402-1410.
[45]. Proudfoot M, Bede P, Turner MR. Imaging Cerebral Activity in Amyotrophic Lateral Sclerosis. *Front Neurol*. 2018;9**:**1148.
[46]. Christidi F, Karavasilis E, Argyropoulos GD*, et al.* Neurometabolic Alterations in Motor Neuron Disease: Insights from Magnetic Resonance Spectroscopy. *J Integr Neurosci*. 2022;21**:**87.
[47]. Bede P, Murad A, Hardiman O. Pathological neural networks and artificial neural networks in ALS: diagnostic classification based on pathognomonic neuroimaging features. *J Neurol.* 2021.
[48]. Bede P, Iyer PM, Finegan E, Omer T, Hardiman O. Virtual brain biopsies in amyotrophic lateral sclerosis: Diagnostic classification based on in vivo pathological patterns. *Neuroimage Clin*. 2017;15**:**653-658.
[49]. Finegan E, Li Hi Shing S, Siah WF*, et al.* Evolving diagnostic criteria in primary lateral sclerosis: The clinical and radiological basis of "probable PLS". *Journal of the Neurological Sciences*. 2020;417**:**117052.
[50]. Finegan E, Siah WF, Shing SLH*, et al.* Imaging and clinical data indicate considerable disease burden in 'probable' PLS: patients with UMN symptoms for 2-4 years. *Data Brief*. 2020**:**106247.

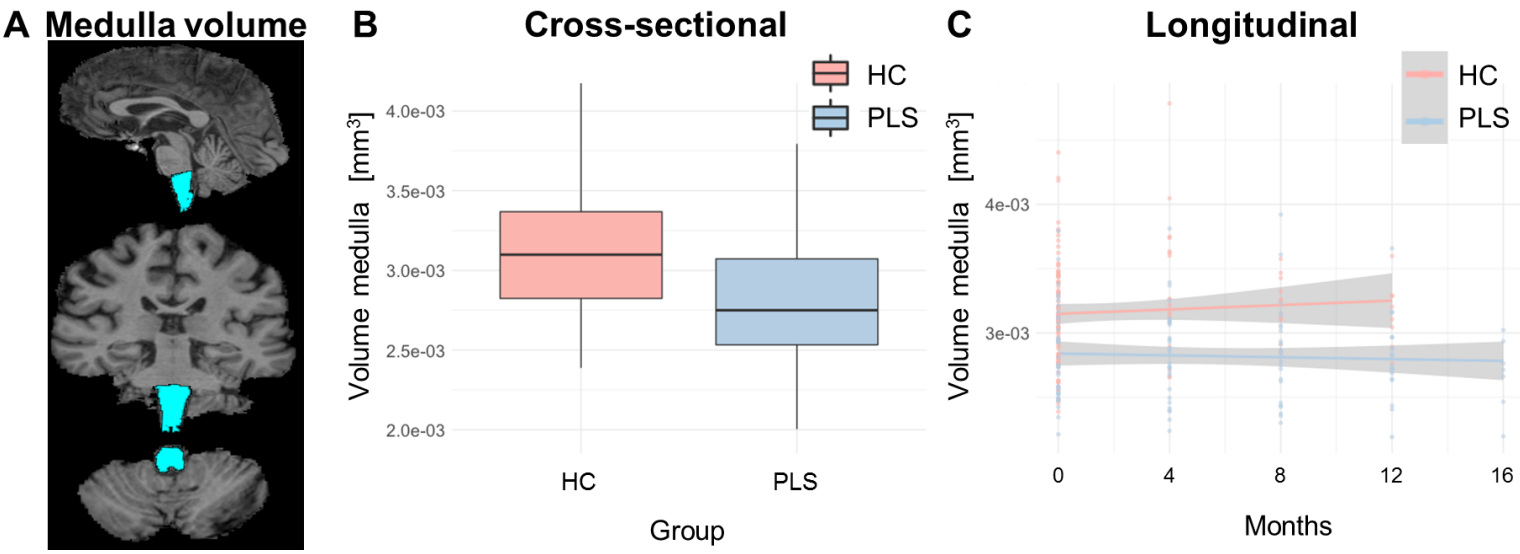

ENE_15725_Fig1_MedVol.tif

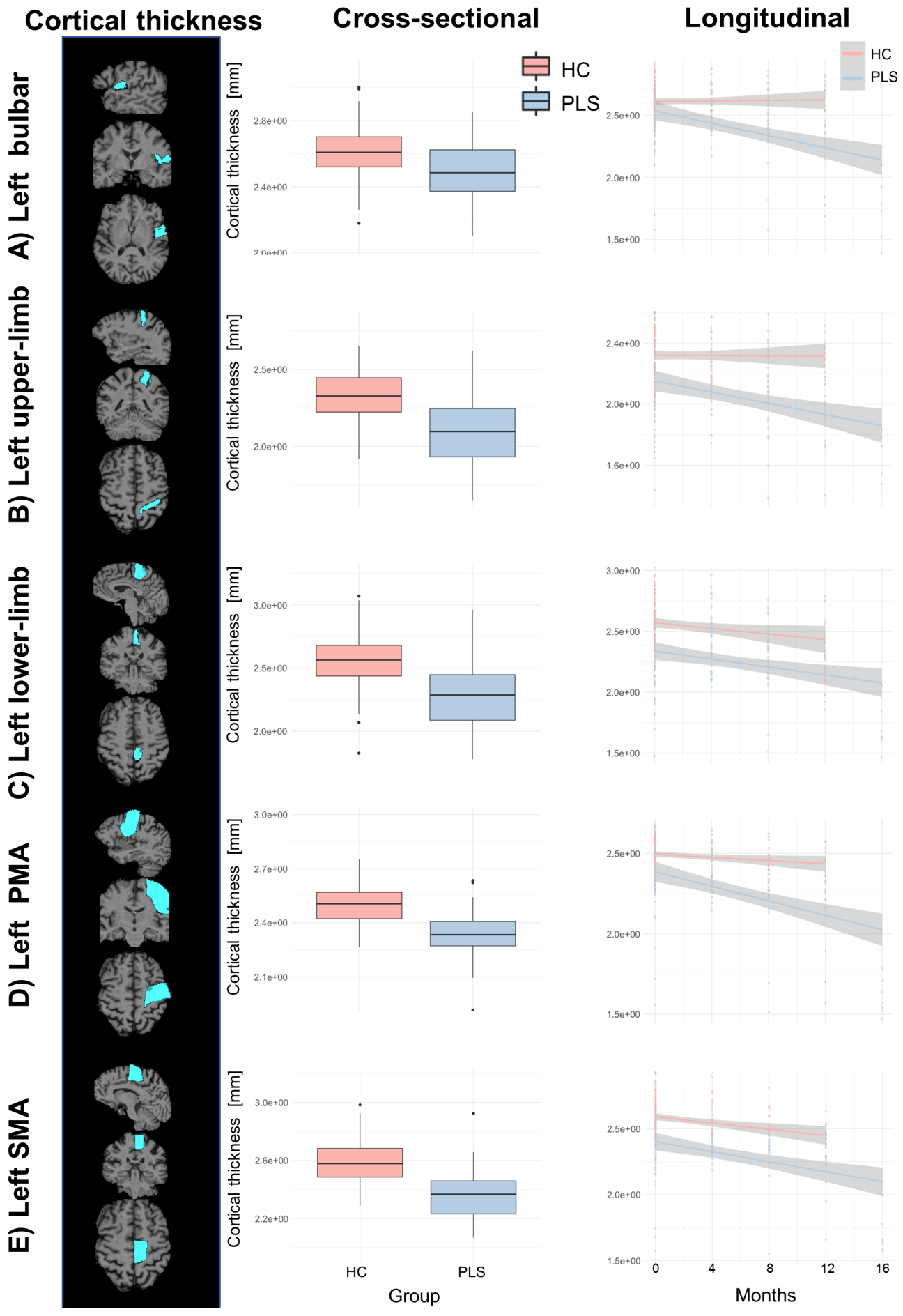

ENE_15725_Fig2_CT.tif

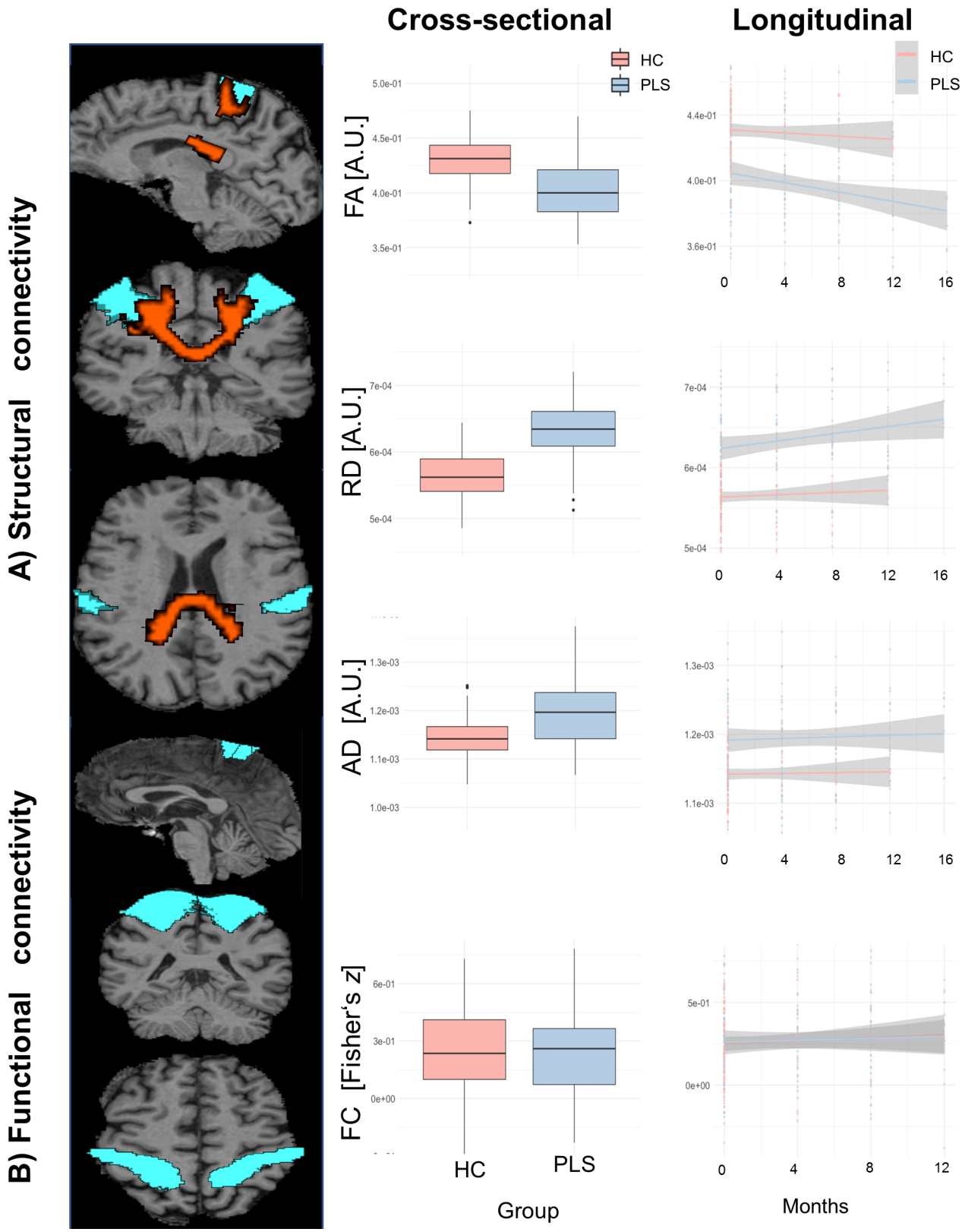

ENE_15725_Fig3_interM1.tif

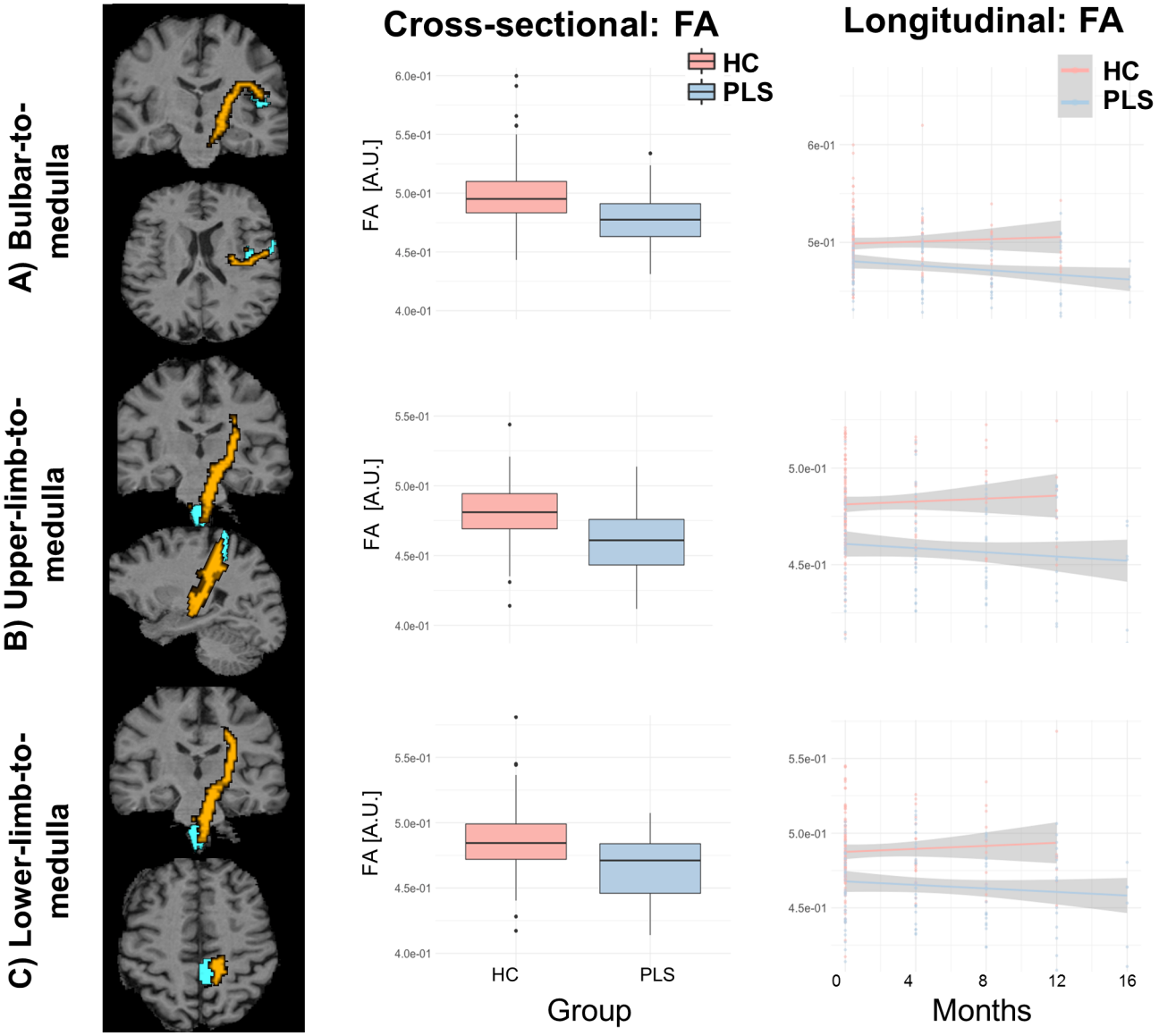

ENE_15725_Fig4_med_cortex.tif

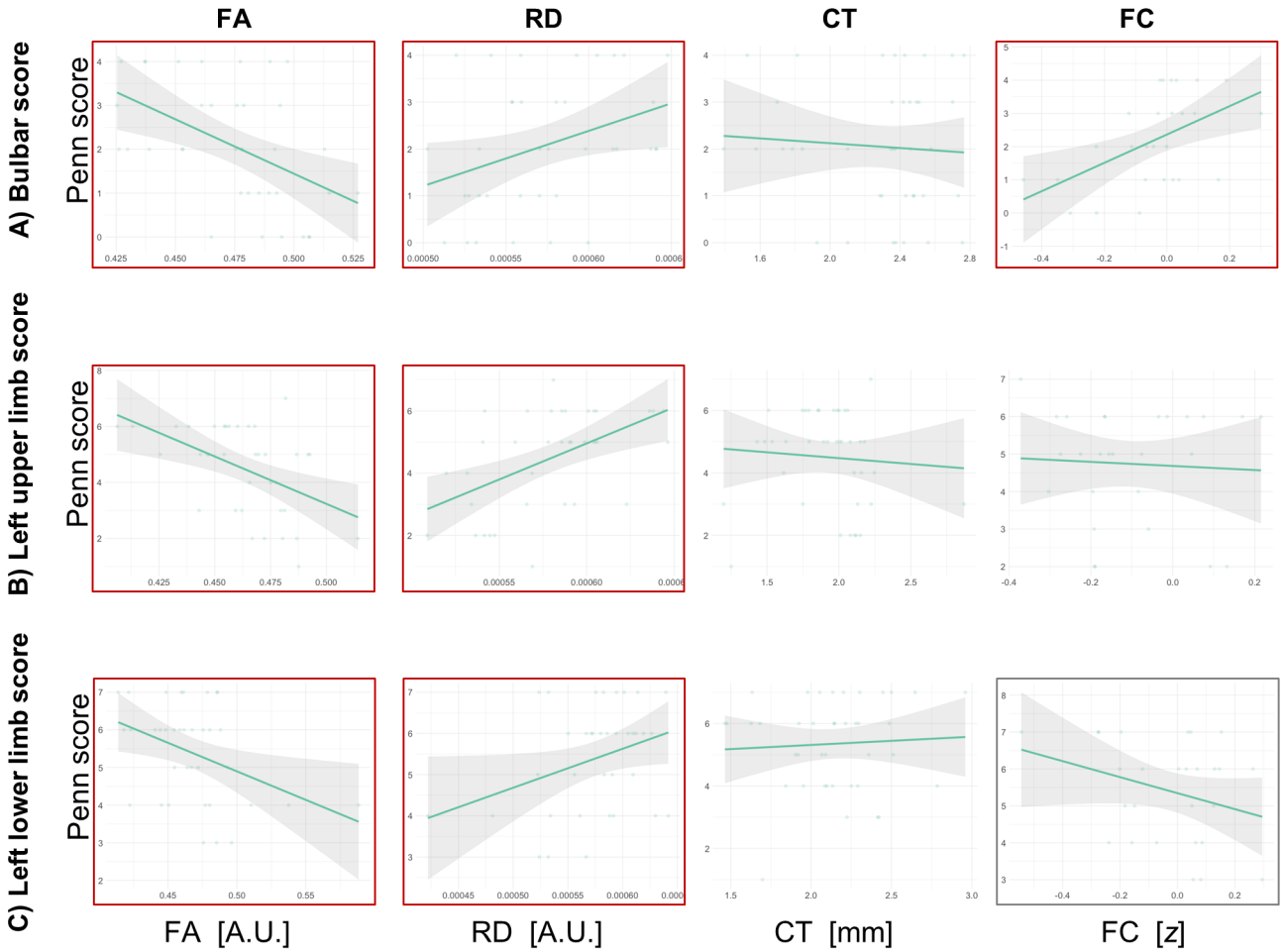

ENE_15725_Fig5_Penn.tif

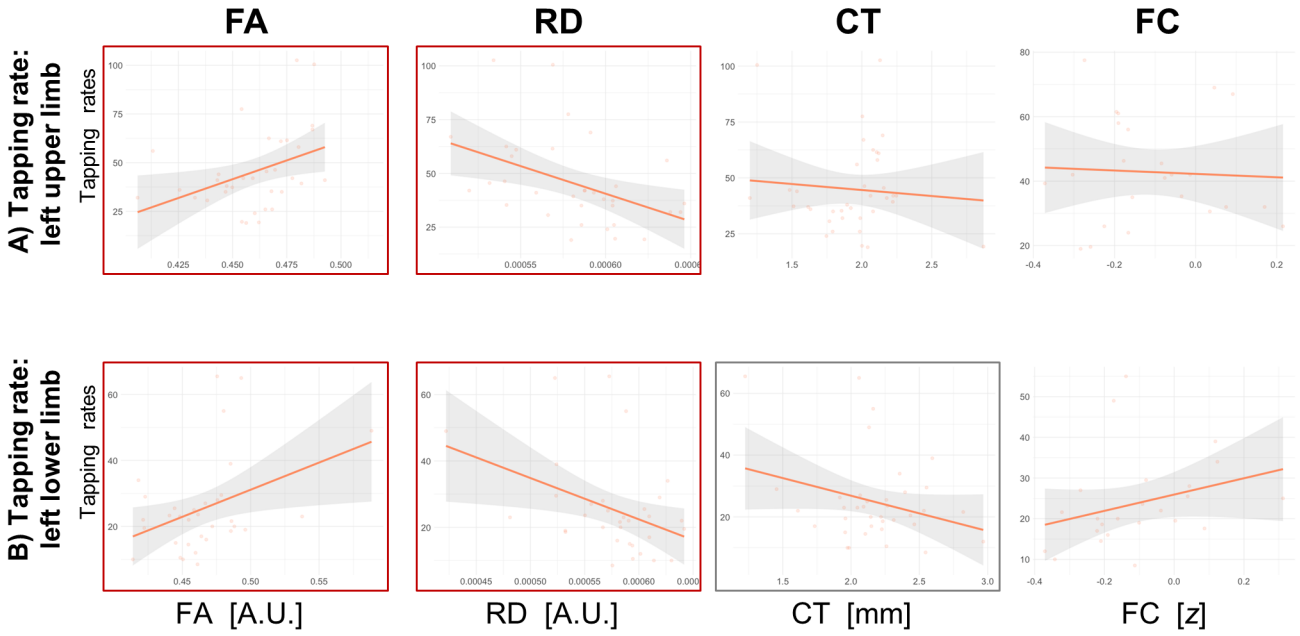

ENE_15725_Fig6_Tap.tif